Nuclear Materials and Energy 41 (2024) 101743

Contents lists available at ScienceDirect

Nuclear Materials and Energy

journal homepage: www.elsevier.com/locate/nme

Impurity behaviour in JET high-current baseline scenario for Deuterium, Tritium and Deuterium-Tritium plasmas

N. Wendler [a,*], A. Chomiczewska [a], W. Gromelski [a], E. Kowalska-Strzęciwilk [a], G. Telesca [a], I. Ivanova–Stanik [a], L. Garzotti [b], D. Van Eester [c], V.K. Zotta [d], D. Frigione [e], F. Rimini [b], G. Pucella [f], JET Contributors[1], The Eurofusion Tokamak Exploitation Team[2]

[a] *IPPLM, Warsaw, Poland*
[b] *UKAEA, Culham Science Centre, Abingdon, United Kingdom*
[c] *LPP-ERM/KMS, Brussels, Belgium*
[d] *Dipartimento di Ingegneria Astronautica, Elettrica ed Energetica, Sapienza Università di Roma, via Eudossiana 18, 00184 Roma, Italy*
[e] *Universita di Roma Tor Vergata, Via del Politecnico 1, Roma, Italy*
[f] *ENEA, Fusion and Nuclear Safety Department, Frascati, Italy*

ARTICLE INFO

Keywords:
Deuterium-Tritium plasmas
JET tokamak
Plasma impurities
Plasma radiation

ABSTRACT

To support future ITER operation, experimental campaigns at the Joint European Torus (JET) with an ITER-like wall (tungsten divertor and beryllium main chamber) in pure deuterium (D), tritium (T) and Deuterium-Tritium (D-T) were performed. One of the most important challenges in recent years was the development of two main scenarios that investigated different approaches to achieve the high fusion power as well as good plasma confinement (Garzotti et al., 2023). The first one, so-called baseline scenario is relying on high plasma current (I_p≈3.5 MA), normalized beta $\beta_N < 2$ and safety factor $q_{95} \approx 3$ (Garzotti et al., 2023). On the other hand, the second one, so-called Hybrid scenario is operating at lower plasma current (flat-top $I_p \leq 2.6$ MA) and density with respect to the baseline, higher normalized beta $\beta_N > 2$ and safety factor $q_{95} \approx 4.8$ (Hobirk et al., 2023).

In this paper we focus on the impurity behaviour analysis for the baseline discharges at $I_p = 3.5$ MA and $B_T = 3.3$ T with D, T and DT plasmas, in which the gas and power waveform were optimized to achieve the best possible performance. In particular, we study the impact of total heating power ($P_{tot} + P_{alpha}$), flat-top gas flow and ELM (edge localized modes) frequency on mid-Z (Nickel (Ni), Copper (Cu)) and high-Z (Tungsten (W)) impurities. In addition, we compared the two best performing pulses of the baseline scenario ($I_p = 3.5$MA, $B_T = 3.3$ T and $P_{in} \approx 35$ MW) in D and DT in order to identify the causes responsible for the increase in radiation during the DT pulse, which led to an early plasma termination. All presented results rely on the data collected by the VUV as well as the bolometry system. Detailed analysis indicates that in the baseline scenario, higher radiation, which is most likely due to the tungsten (W), is observed for T and DT plasmas in comparison to D. Moreover, for the two best performing baseline pulses, tomographic reconstructions show that the radiated power density is mainly emitted from the low field side (LFS) of the plasma and W does not accumulate in the plasma center (Telesca et al., 2024).

Introduction

One of the main scientific goals of the second major JET Deuterium-Tritium experimental campaign (DTE2), which took place in 2021 was to demonstrate a steady plasma discharges with high fusion power ($P_{fus} \geq 10$ MW) for a duration of 5 s. To reach this aim, two main ELMy H-mode experiments in JET-ILW were prepared – the so-called baseline scenario [1], as well as the Hybrid scenario [2,4].

* Corresponding author.
E-mail address: natalia.wendler@ifpilm.pl (N. Wendler).

[1] See the author list of “Overview of T and D-T results in JET with ITER-like wall” by C.F. Maggi et al. to be published in Nuclear Fusion special issue: Overview and summary papers from the 29th Fusion Energy Conference (London, UK, 16-21 October 2023).

[2] See the author list of “Progress on an exhaust solution for a reactor using EUROfusion multi-machines capabilities” by E. Joffrin et al. to be published in Nuclear Fusion Special Issue: Overview and Summary Papers from the 29th Fusion Energy Conference (London, UK, 16-21 October 2023).

https://doi.org/10.1016/j.nme.2024.101743
Received 10 May 2024; Received in revised form 9 August 2024; Accepted 19 September 2024
Available online 20 September 2024

The baseline scenario, one of the foreseen for ITER, is operating at high toroidal field and plasma current ($I_p \geq 3.5$ MA)[5]. Moreover, baseline plasmas are characterized by relatively low normalized beta ($\beta_N \sim 2$) compared to the parallel optimized hybrid scenario, as well as edge safety factor $q_{95} \sim 3$. Additionally, pulses in baseline regime typically exhibiting compound edge localized modes (ELMs) and relay on high auxiliary heating power, namely, ~4 MW of ICRH and >32 MW of NBI [1], as well as pacing pellet injection for ELM triggering, high-Z impurity flushing and density control.

The baseline scenario, similarly as Hybrid scenario, is exposed to high-Z impurities, primarily W, which originates from the divertor targets and can lead to unacceptable disruption [1,6,7]. It is worth noting that, while the baseline scenario has been successfully developed for high performance in D for 5 s, it has not been possible to sustain this scenario in T and DT for more than 2–3 s [1]. Therefore, investigation of impurity behaviour and understanding of the causes that led to an uncontrolled increase of radiated power, were one of the crucial issues.

In this study, we concentrate on impurity analysis in which, mid-Z and high-Z impurities behaviour, as well as plasma radiation are compared within different plasmas mixtures, namely D, T and DT. Furthermore, as part of this research, the impact of total heating power, flat-top gas flow and ELMs frequency on plasma impurities was investigated. Additionally, the two best performing pulses in baseline regime, one in D (#96482), and the other in DT (#99948) plasmas were also compared in terms of possible differences in impurities behaviour, to identify the causes that lead to an uncontrolled radiation increase in plasma mixtures with the higher isotope mass.

The results of this study are primarily based on data collected by the VUV survey spectrometer [8,9] (known as KT2 at JET) as well as bolometry diagnostic [10]. Data from the first system is typically used for quantitative measurement of mid-Z impurities like Nickel or Copper. Their concentrations in the plasmas (c_Ni and c_Cu), presented in this work, were estimated using the method described in detail in [11]. Moreover, using data from the above mentioned spectrometer, it was possible to estimate the intensity of different W ionization stages (W^{14+}–W^{35+}) from quasicontinuum spectra in VUV [12], defined in this paper as I_W. The determination of this parameter is important due to the lack of data from the XUV diagnostic (known as KT7/3 system at JET) and SXR cameras, which are normally used for studies relating to quantitative analysis of W [13–15]. Unfortunately, due to the high neutron rate in the DT and T plasmas, both diagnostic systems have been disconnected. In turn, the tomographic reconstruction of the radiated power density have been obtained from bolometry measurements. However, it is important to note that some of the baseline pulses discussed in this work involved the use of Tritium Introduction Modules (TIM)15, which led to contaminated signals in the horizontal bolometer camera. To address this, the contribution from TIM15 was removed by progressively reducing the signal levels on the horizontal camera until the reconstruction output accurately balanced the data from both cameras [16].

Impurity analysis for the high-current baseline pulses in Deuterium, Deuterium-Tritium and Tritium plasmas

The development of the high-current baseline scenario on JET before and during DTE2 has led to the achieving high fusion performance in D for 5 s, whereas in DT and T plasmas, the same scenario was sustained only for 3 s. and 1–2 s., respectively [1,5]. According to Ref. [1], the main difficulties in sustaining DT and T plasmas can be explained by different ELMs activity as well as an increased electron density. Namely, in D plasmas, the radiated power mostly remains constant because inter-ELM particle transport as well as ELM activity provide a stationary plasma density, which, most importantly, does not increase over time. In turn, in T and DT plasmas, where the reduced particle transport is observed, the plasma density builds up between ELMs. In these cases, the ELM activity is insufficient to flush high-Z impurities, such as tungsten, resulting in a gradual increase in plasma radiation over time. Consequently, it can be stated that both electron density and ELMs activity affect impurities differently, depending on the plasma isotope mass [3]. For this reason, in this part of work, we concentrate on the analysis of impurity behaviour, which has been performed for the set of baseline pulses in D, DT and T plasmas, obtained during DTE2 experimental campaign, to investigate possible differences for various plasma isotopic compositions in the context of plasma radiation. In the analysed pulses, which were performed at 3.5 MA, values of particular plasma parameters were averaged over t = 9 s. to t = 10 s. (in the time window with a stable plasma conditions).

At the beginning of this study, the total radiated power $P_{rad,total}$ as well as plasma radiation at the edge $P_{rad,edge}$ (estimated using channel 2 of the vertical bolometer camera, which was unaffected by TIM15), were compared across various plasma mixtures. As is shown in Fig. 1. a linear increase of $P_{rad,total}$ with auxiliary heating was observed for all plasma compositions studied, namely D, DT and T. Moreover, it can be seen that DT and T plasmas are characterised by higher radiation compared to D pulses. Comparable trends were observed for the $P_{rad,edge}$ (see Fig. 1). What is worth emphasizing, differences in radiated power values between pure T discharges and plasmas mixtures with DT and D result from different electron density profiles. In the next step of analysis, mid-Z impurities concentration (c_Ni and c_Cu), as well as I_W were investigated.

As is presented in Fig. 2, I_W is well correlated with the $P_{rad,total}$ and $P_{rad,edge}$ showing an increasing trend with auxiliary heating in all plasma mixtures. In the case of mid-Z impurities, the highest c_Ni and c_Cu were observed in T plasmas (Fig. 2). However, no significant increase in their values with increasing total power was observed. In turn, the estimated concentrations of other mid-Z elements, such as Fe and Mo, were found to be negligible. Moreover, the results presented in this section, confirm that the increase in plasma radiation and impurity concentration in plasma mixtures with higher isotope mass is associated with a weakened

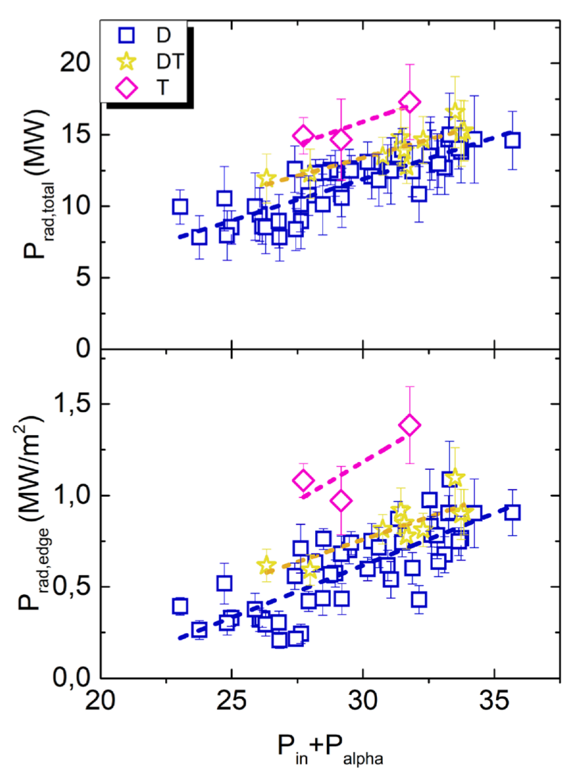

Fig. 1. The total radiated power $P_{rad,total}$ (on the top) and the the edge line averaged radiation $P_{rad,edge}$ (on the bottom) from a vertical bolometer channel as a function of the sum of input and the alpha particles powers for D, DT and T plasmas. Dashed lines indicate linear fit to particular data sets.

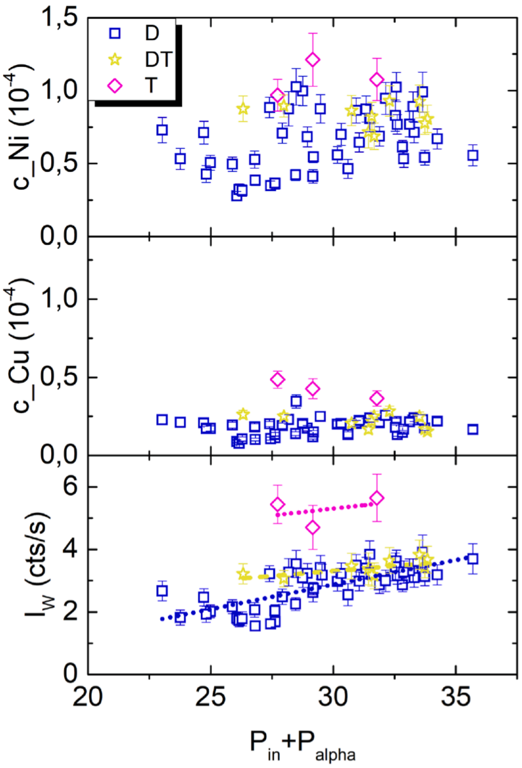

Fig. 2. From the top: The nickel concentration c_Ni, the copper concentration c_Cu and the intensity of tungsten I_W as a function of the sum of input and the alpha particles powers for D, DT and T plasmas. Dashed lines indicate linear fit to particular data sets.

ELM activity and a different electron density at the plasma edge. Namely, as can be seen in Fig. 3, lower f_{ELM} in T plasmas compared to DT and D may result in higher plasma radiation, since the lower f_{ELM} in baseline pulses typically lead to less effective impurity flushing [3,6].

Additionally, because plasma radiation (P_{rad}) is directly proportional to electron density [3], higher $n_{e,edge}$ (Fig. 4) in T plasmas results in higher values of $P_{rad,edge}$. On the other hand, as shown in Fig. 2, the higher observed values of c_Ni and c_Cu, measured closer to the edge in T pulses, may indicate a greater presence of Ni and Cu impurities in plasmas with higher isotope mass. This is because, with both higher values of $n_{e,edge}$ and impurities concentrations (c_Ni and c_Cu) measured

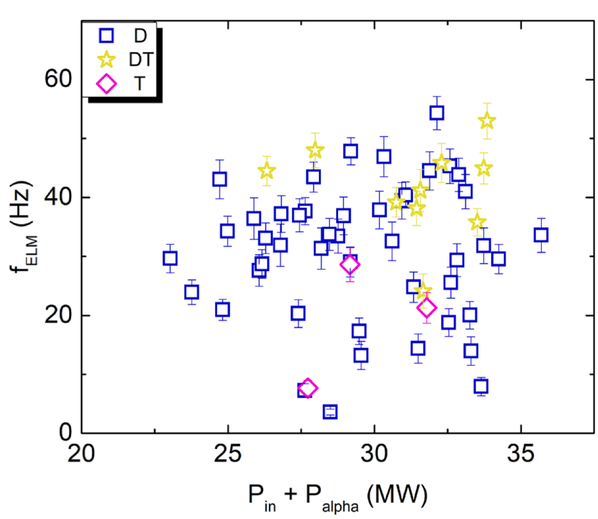

Fig. 3. The ELMs frequency f_{ELM} as a function of the sum of input and the alpha particles powers for D, DT and T plasmas.

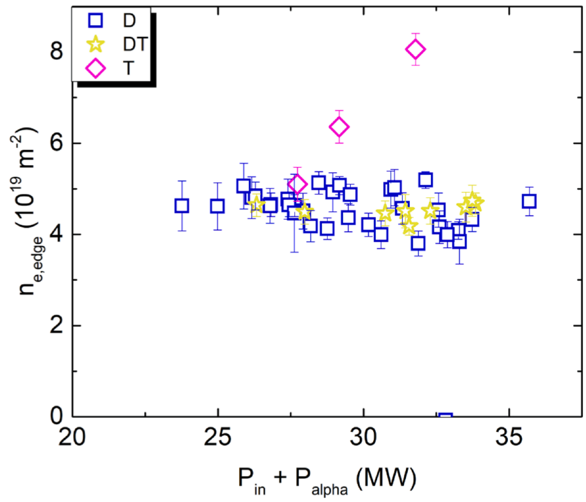

Fig. 4. The line integrated edge density $n_{e,edge}$ as a function of the sum of input and the alpha particles powers for D, DT and T plasmas.

at the plasma edge, higher densities of Cu and Ni are also expected. Furthermore, experimental observations indicate that a decrease in plasma radiation (both $P_{rad,total}$ and $P_{rad,edge}$), impurities concentrations, as well as I_W is linked to an increase in flat-top gas flow, what is presented on Fig. 5 and Fig. 6, respectively. This could be explained by the fact that the higher gas flow injection rate usually increases the ELM frequency (f_{ELM}), as well as a turbulent transport. As a result, more W can be flushed out [6] and reduced plasma radiation may be observed. For this reason, the additional gas in the D baseline plasmas was typically used to control the ELMs, and prevent uncontrolled radiation.

In the context of the analysis presented in this section, it should be also mentioned that its primary constraint is the small number of T

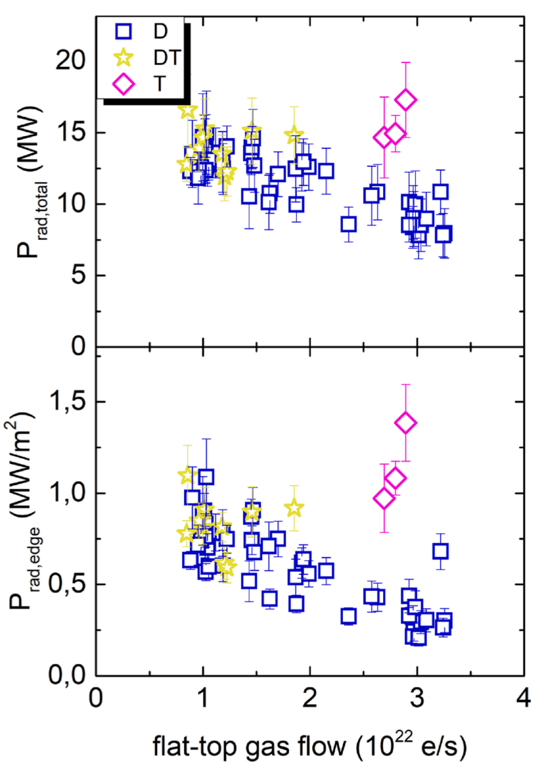

Fig. 5. The total radiated power $P_{rad,total}$ (on the top) and the the edge line averaged radiation $P_{rad,edge}$ (on the bottom) from a vertical bolometer channel as a function of the flat-top gas flow for D, DT and T plasmas.

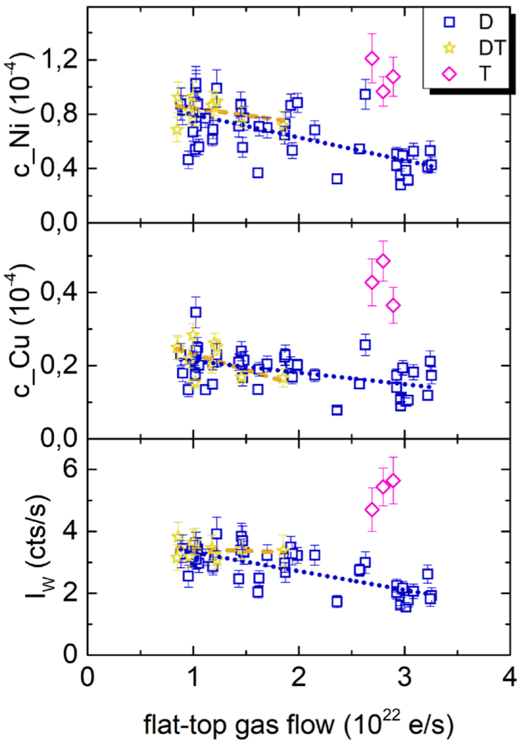

Fig. 6. From the top: The nickel concentration c_Ni, the copper concentration c_Cu and the intensity of tungsten I_W as a function of the flat-top gas flow for D, DT and T plasmas. Dashed lines indicate linear fit to particular data sets.

discharges compared to DT and D pulses. However, the results presented here show that T pulses in most cases forms a distinctly separate group from DT and D plasmas, even when considering measurement uncertainties.

Comparison of the two best performing baseline pulses in Deuterium and Deuterium-Tritium plasmas

As was mentioned in Section 2, one of the main reasons for the development of the baseline scenario in DT and T was to investigate and mitigate possible isotope effects, which can influence, among other things, the plasma radiation. Therefore, this section of the work focuses primarily on the analysis of impurities in the two best performing pulses obtained in D and DT at $I_p = 3.5$ MA with a magnetic field strength of ≈3.35 T and with auxiliary heating power $P_{in} \approx 35$ MW (including $P_{NBI} \approx 30$ MW and $P_{ICRH} \approx 5$ MW). In this study, DT plasmas differ from D in higher electron density and the plasma energy. However, the core temperatures of T_{i0} and T_{e0} in both pulses were comparable, approximately 7 keV, which is typical for this type of plasma scenario. Furthermore, as is well known, a high plasma current implies high electron density. However, despite the fact that both investigated pulses were performed at the same I_p, the electron density in DT plasmas was increasing continuously, whereas the n_e in D was nearly constant during the entire pulse (see Fig. 7). This can be explained by the fact that, in the case of baseline discharges, the enhanced particle confinement due to the higher effective isotope mass results in a greater pedestal and volume-averaged density in DT compared to D [1]. What is also particularly relevant, the increase in electron density in the DT plasmas was accompanied by an increase in time of $P_{rad,total}$ and $P_{rad,edge}$. Excessively high level of radiation finally led to the disruption at t ≈ 11.5 s., approximately three seconds after achieving the maximum of the auxiliary heating. Therefore, it was crucial to identify which plasma impurities had a decisive influence on the observed plasma radiation, and equally importantly, what was their source. Fig. 8 shows Ni and Cu

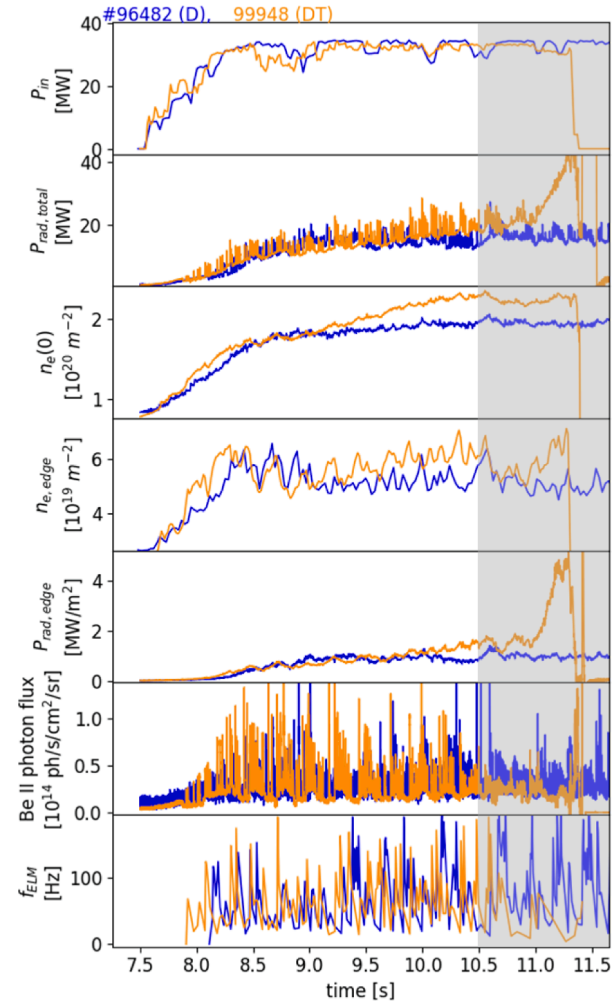

Fig. 7. Time traces for D (#96482) and DT (#99948) pulses, showing from the top: heating power, the total radiated power, the line integrated density, the line integrated edge density, the edge line averaged radiation from a vertical bolometer channel, The Be II photon flux, the ELM frequency. The grey vertical bar denotes the time range where ELM activity is lost in DT plasmas.

concentrations, as well as intensity of W, which were measured close to the plasma edge. As can be seen, in DT plasmas, all these parameters start to gradually increase from around t ≈ 9.5 s., after which they achieve their highest values at t ≈ 11.5 s. that corresponds to the time of the plasma disruption. Moreover, the behaviour of c_Ni, c_Cu and I_W in DT pulse is well correlated with $P_{rad,edge}$ and $P_{rad,total}$. In contrast, in the case of D, the aforementioned parameters remain almost constant for the entire pulse without leading to early plasma termination. Furthermore, as it can be also observed in Fig. 9, c_Ni and c_Cu, which were estimated at mid-radius plasma region, stay stable over the entire pulses in both D and DT plasmas. This may indicate that impurities which have contributed to $P_{rad,total}$ and finally led to the premature stop of the plasma, were located in the mantle region.

In order to verify these results, 2D Tomographic reconstructions of the radiation density were additionally performed for the following time points, $t_1 \approx 9$ s., $t_2 \approx 10$ s. and $t_3 \approx 11$ s., which correspond to different levels of the observed $P_{rad,total}$. As can be seen from Fig. 10, in D plasmas, the intensity of the radiation on the LFS does not change significantly over time, whereas in DT plasmas a gradual increase can be observed. Additionally, for the time point shortly before plasma disruption in DT, namely t = 11 s, the radiation power density was at least twice that of D plasmas. Moreover, presented reconstructions show that the radiated power density, in both plasma mixtures were mainly emitted from the

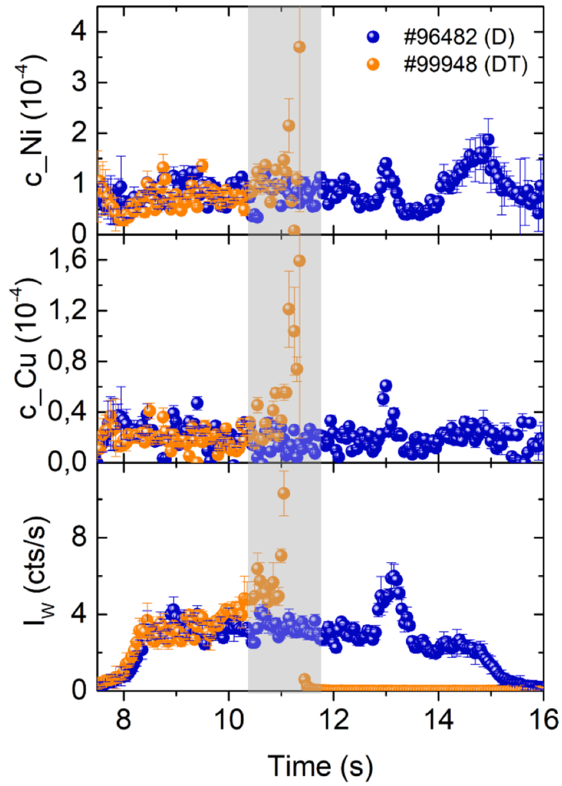

Fig. 8. Time traces showing from the top: the nickel concentration c_Ni, the copper concentration c_Cu and the intensity of tungsten I_W measured at plasma edge for D and DT plasmas.

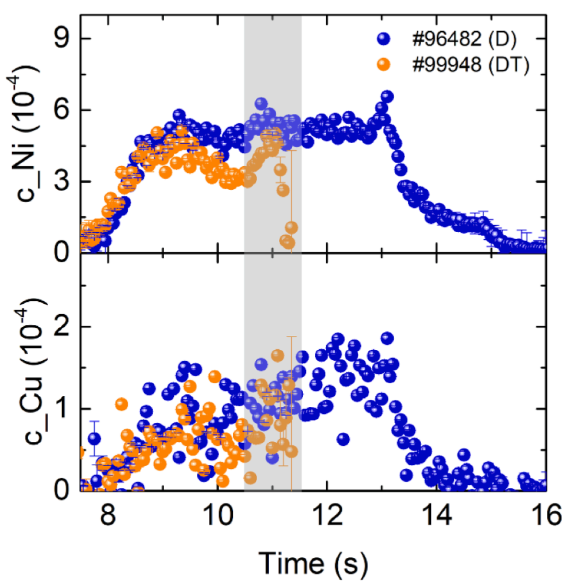

Fig. 9. Time traces showing from the top: the nickel concentration c_Ni, the copper concentration c_Cu measured at mid-radius for D and DT plasmas.

LFS of the plasma, which is consistent with the results from VUV spectrometer regarding c_Ni, c_Cu and I_W. Such localization of the heavy impurities, on the outboard mid-plane of the LFS, results from the toroidal rotation, as is described in [5,6]. Additionally, it is worth mentioning that, according to investigation of the MHD data described in [3], TM (tearing modes) mode evolution in both analysed pulses is different, however it does not depend on the different level of $P_{rad,tot}$.

Given the above, it can be stated that in DT plasmas, the higher

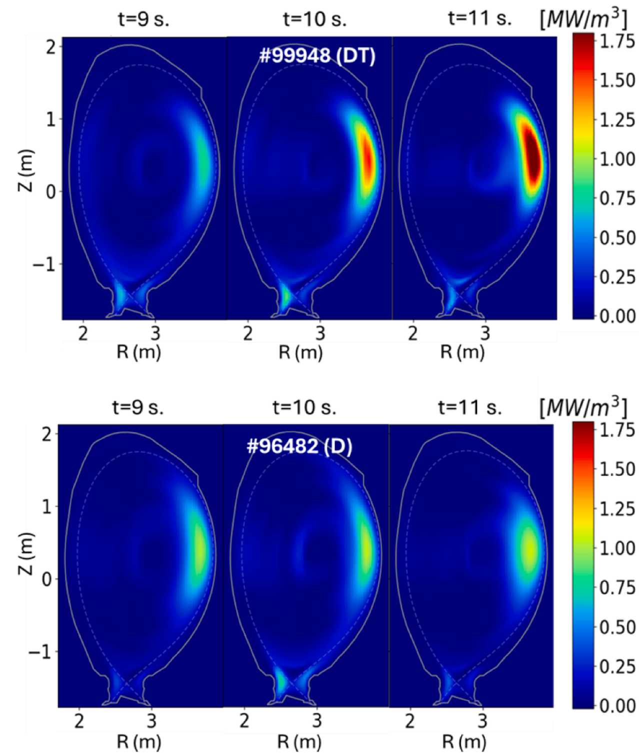

Fig. 10. Bolometry reconstructions for DT (#99948) and D (#96482) pulses at t = 9 s., t = 10 s. and t = 11 s.

electron density (which results from enhanced particle confinement) was associated with higher plasma radiation ($P_{rad,total}$ and $P_{rad,edge}$), as well as less frequent ELMs (see the grey vertical area on Fig. 7), which led to inefficient impurity flushing. As experimental observations indicate, the combination of these events can result in a loss of stationarity and a radiative collapse in the DT plasma.

Conclusion

During the second JET Deuterium-Tritium experimental campaign with a substantial tritium concentration, the baseline scenario pulses have been optimised and tested. The experiments and analyses that have been performed at high field and current, showed that for plasma mixtures with higher isotope mass, controlling plasma radiation is more challenging. For this reason, study of the plasma impurities and radiation, was one of the most important tasks. According to the impurity analysis, DT and T plasmas exhibiting higher impurities content and intensity of W in comparison to D pulses, which is in line with observations on $P_{rad,total}$ and $P_{rad,edge}$. Furthermore, it has been noted that a higher flat-top gas flow rate, results in a decrease of impurities content and as a consequence can lead to the reduction of excessive plasma radiation. In turn, observations from a comparison of the two best performing pulses, one in D, and the other in DT, indicate that plasma mixtures with higher isotope mass, features enhanced particle confinement and, as a result, a higher electron density compared to D. Moreover, higher n_e values is accompanied by increased plasma radiation, which, together with a less effective ELM impurity flushing, may lead to an early termination of the pulse. In addition, it has been found that impurities in the baseline plasmas, mainly accumulate on the LFS. This observation is confirmed by data from both, the VUV spectrometer, as well as the Bolometry diagnostic. In this regard, controlling the electron density and ELMs activity appears to be a key issue in achieving a stable and high-performance baseline plasma.

CRediT authorship contribution statement

N. Wendler: Writing – original draft, Investigation, Formal analysis, Conceptualization. **A. Chomiczewska:** Methodology, Investigation. **W. Gromelski:** Software, Resources. **E. Kowalska-Strzęciwilk:** Resources. **G. Telesca:** Writing – review & editing, Investigation. **I. Ivanova–Stanik:** Investigation. **L. Garzotti:** Investigation. **D. Van Eester:** Investigation. **V.K. Zotta:** Investigation, Writing – review & editing. **D. Frigione:** Investigation. **F. Rimini:** Investigation. **G. Pucella:** Investigation.

Declaration of competing interest

The authors declare the following financial interests/personal relationships which may be considered as potential competing interests: Natalia Wendler reports financial support was provided by Institute of Plasma Physics and Laser Microfusion. If there are other authors, they declare that they have no known competing financial interests or personal relationships that could have appeared to influence the work reported in this paper.

Data availability

Data will be made available on request.

Acknowledgements

This scientific paper has been published as part of the international project co-financed by the Polish Ministry of Science and Higher Education within the programme called 'PMW' for 2021-2023.

This work has been carried out within the framework of the EUROfusion Consortium, funded by the European Union via the Euratom Research and Training Programme (Grant Agreement No 101052200 — EUROfusion). Views and opinions expressed are however those of the author(s) only and do not necessarily reflect those of the European Union or the European Commission. Neither the European Union nor the European Commission can be held responsible for them.

References

[1] L. Garzotti et al., Development of high-current baseline scenario for deuterium-tritium high fusion performance at JET, 29th IAEA Fusion Energy Conference, 16-21 October 2023, London, United Kingdom.
[2] J. Hobirk et al., The JET Hybrid scenario in D, T and D-T, 2023 Nucl. Fusion 63.
[3] G. Telesca et al., COREDIV simulations of D and D-T high current-high power Baseline pulses in JET ITER-Like Wall, Nucl. Fusion 64 (2024) 066018 (14pp).
[4] J. Hobirk et al, Improved confinement in JET hybrid discharges, 2012 Plasma Phys. Control. Fusion 54 095001.
[5] D. Van Eester, RF power as key contributor to high performance "baseline" scenario experiments in JET DD and DT plasmas in preparation for ITER, AIP Conf. Proc. 2984 (2023) 030004.
[6] A.R. Field, The impact of fuelling and W radiation on the performance of high-power, ITER-baseline scenario plasmas in JET-ILW, Plasma Phys.Control. Fusion 63 (2021) 095013.
[7] M. Maslov, et al., Nuclear Fusion 63 (2023) 112002.
[8] I.H. Coffey, R. Barnsley, Rev. Sci. Instrum. 75 (2004)3737.
[9] K. D. Lawson, I. H. Coffey, J. Zacks, M. F. Stamp, JET-EFDA contributors, An absolute sensitivity calibration of the JET VUV SPRED spectrometer, 2009 JINST 4 P04013.
[10] A. Huber, et al., Upgraded bolometer system on JET for improved radiation measurements, Fusion Eng. Design 82 (2007) 1327–1334.
[11] A. Czarnecka, et al., Determination of metal impurity density, ΔZeff and dilution on JET by VUV emission spectroscopy, Plasma Phys. Control. Fusion 53 (2011) 035009.
[12] K.D. Lawson, et al., Plasma Phys. Control. Fusion 63 (2021) 105001.
[13] N. Krawczyk et al., Application of the VUV and the soft x-ray systems on JET for the study of intrinsic impurity behaviour in neon seeded hybrid discharges, Review of Scientific Instruments 89(2018) 10D131W.
[14] A Czarnecka et al., Analysis of metallic impurity content by means of VUV and SXR diagnostics in hybrid discharges with hot-spots on the JET-ITER-like wall poloidal limiter, Plasma Phys. Control. Fusion 61 (2019) 085004 W.
[15] T. Pütterich, et al., Observations on the W-transport in the core plasma of JET and ASDEX Upgrade Plasma Phys. Control. Fusion 55 (2013) 124036 W.
[16] P. Carvalho, private communication (2023).